The $[Mn_2(2\text{-}OHsalpn)_2]^{2-,1-,0}$ System: An Efficient Functional Model for the Reactivity and Inactivation of the Manganese Catalases

Andrew Gelasco, Stephan Bensiek, and Vincent L. Pecoraro*

Department of Chemistry, The University of Michigan, Ann Arbor, Michigan 48109-1055

Received January 7, 1998

The complexes $[Mn(2\text{-}OH(X\text{-}sal)pn)]_2^{n-}$ (where X = 5-OCH_3, H, 5-Cl, 3,5-diCl, or 5-NO_2 and where $n = 0$ or 2) are shown to be excellent hydrogen peroxide disproportionation catalysts in acetonitrile. When carried out in an open vessel, the reaction can occur for over 5000 turnovers without an indication of catalyst decomposition. The disproportionation reaction cycles between the $[Mn^{III}(2\text{-}OH(X\text{-}sal)pn)]_2$ and the $[Mn^{II}(2\text{-}OH(X\text{-}sal)pn)]_2^{2-}$ oxidation levels. All derivatives show saturation kinetics with the highest k_{cat} (21.9 ± 0.2 s^{-1}) observed for the $[Mn^{III}(2\text{-}OH(5\text{-}Clsal)pn)]_2$ dimer and the optimal k_{cat}/K_M (990 ± 60 $s^{-1}\cdot M^{-1}$) observed for the $[Mn^{III}(2\text{-}OHsalpn)]_2$. The first step of the reaction is proposed to be the binding of peroxide to the $[Mn^{III}(2\text{-}OH(X\text{-}sal)pn)]_2$ through an alkoxide shift to form a ternary intermediate $\{[Mn^{III}(2\text{-}OH(X\text{-}sal)pn)]_2(H_2O_2)\}$. We propose that the turnover-limiting step is the oxidation of peroxide from this intermediate. The binding efficiency of the peroxide is dependent on the phenyl-ring substitution with the derivatives donating the most electrons having the highest affinity for the substrate. Studies with isotopically labeled H_2O_2 indicate that protons are important in the turnover-limiting step of the reaction and that the O−O bond is not cleaved during peroxide oxidation. In a closed vessel, the product dioxygen will oxidize $[Mn^{II}(2\text{-}OH(5\text{-}NO_2sal)pn)]_2^{2-}$ to $[Mn^{II/III}(2\text{-}OH(5\text{-}NO_2sal)pn)_2]^-$, and this species can then be stoichiometrically oxidized by hydrogen peroxide to give $[Mn^{III/IV}(2\text{-}OH(5\text{-}NO_2sal)pn)_2(\mu_2\text{-}O)_2]^-$. This di-$\mu_2$-oxobridged species is catalytically incompetent; however, addition of hydroxylamine hydrochloride restores catalytic activity. The relationship of this catalytic disproportionation of hydrogen peroxide and inactivation of the catalyst will be used to define a model for similar reactions observed for the *Lactobacillus plantarum* Mn catalase.

Similar to the heme catalases, the manganese catalases disproportionate hydrogen peroxide according to eq 1.

$$2H_2O_2 \rightarrow O_2 + 2H_2O \quad (1)$$

These manganese enzymes have been isolated from three different bacteria: *Lactobacillus plantarum*,[2,3] *Thermus thermophilus*,[4] and *Thermoleophilium album*.[5] Through activity studies,[5−7] spectroscopy,[8−11] and X-ray crystallographic structural analysis,[12−14] all three enzymes appear to be very similar. The dinuclear manganese center probably cycles between the $Mn^{II}_2 \leftrightarrow Mn^{III}_2$ oxidation levels during the normal catalytic cycle with at least two proposed mechanisms for the catalytic disproportionation of hydrogen peroxide by the Mn catalases having been presented.[7] Evidence for this cycle has been shown by the identical steady-state kinetics for the oxidized (Mn^{III}_2) and reduced (Mn^{II}_2) forms of *T. thermophilus*[6] and by observation of changes in XANES spectra during turnover of the *L. plantarum* enzyme.[15] Both the *L. plantarum*[7] and *T. thermophilus*[6] enzymes exhibit substrate saturation kinetics and show no inhibition by hydrogen peroxide even at high substrate concentrations. This lack of substrate inhibition is in contrast to original observations that all three known Mn catalases were inhibited at peroxide concentrations as low as 0.1 M.[5,7,13]

Hydroxylamine which can be used for preparing the fully reduced (Mn^{II}_2), the active enzyme form of the catalase, is a good reducing agent. If, however, hydrogen peroxide is added to the enzyme while hydroxylamine is present, there is a rapid conversion to a catalytically inactive, superoxidized form. EPR[10] and EXAFS spectroscopies[16] revealed that this inactive enzyme contains a dioxo-bridged $Mn^{III/IV}$ dinuclear metal center, and magnetic circular dichromism (MCD) studies have suggested, on the basis of a comparison to model compounds, that

(1) Gelasco, A.; Pecoraro, V. L. *J. Am. Chem. Soc.* **1993**, *115*, 7928−7929.
(2) Kono, Y.; Fridovich, I. *J. Biol. Chem.* **1983**, *258*, 6015−6019.
(3) Kono, Y. *J. Biol. Chem.* **1983**, *258*, 13646−13648.
(4) Barynin, V. V.; Grebenko, A. I. *Dokl. Akad. Nauk SSSR* **1986**, *286*, 461−464.
(5) Algood, G. S.; Perry, J. J. *J. Bacteriol.* **1986**, *168*, 563−567.
(6) Shank, M.; Barynin, V. V.; Dismukes, G. C. *Biochemistry* **1994**, *33*, 15433−15436.
(7) Penner-Hahn, J. E. In *Manganese Redox Enzymes*; Pecoraro, V. L., Ed.; VCH Publishers: New York, 1992; pp 29−45.
(8) Waldo, G. S.; Fronko, R. M.; Penner-Hahn, J. E. *Biochemistry* **1991**, *30*, 10486−10490.
(9) Khangulov, S. V.; Voyevodskaya, N. V.; Barynin, V. V.; Grebenko, A. I.; Melik-Adamyan, V. R. *Biofizika* **1987**, *32*, 960−966.
(10) Fronko, R. M.; Penner-Hahn, J. E.; Bender, C. J. *J. Am. Chem. Soc.* **1988**, *110*, 7554−7555.
(11) Khangulov, S. V.; Goldfeld, M. G.; Gerasimenko, V. V.; Andreeva, N. E.; Barynin, V. V.; Grebenko, A. I. *J. Inorg. Biochem.* **1990**, *40*, 279−292.
(12) Vainshtein, B. K.; Melik-Adamyan, W. R.; Barynin, V. V.; Vagin, A. A. In *Progress in Bioorganic Chemistry and Molecular Biology*; Ovchinnikov, Y. A., Ed.; Elsevier Science Publishers: New York, 1984; pp 117−125.
(13) Barynin, V. V.; Vagin, A. A.; Melik-Adamyan, V. R.; Grebenko, A. I.; Khangulov, S. V.; Popov, A. N.; Andrianova, M. E.; Vainshtein, B. K. *Dolk. Akad. Nauk. SSSR* **1986**, *288*, 877−880.
(14) Barynin, V. V., personal communication.
(15) Waldo, G. S.; Penner-Hahn, J. E. *Biochemistry* **1995**, *34*, 4.
(16) Waldo, G. S.; Fronko, R. M.; Penner-Hahn, J. E. *Biochemistry* **1991**, *30*, 10486−10490.

S0020-1669(98)00022-6 CCC: $15.00
Published on Web 06/11/1998

the core contains a third bridge[17] (possibly carboxylate). These results clearly indicate a structural rearrangement of the dinuclear core of the enzyme upon deactivation of the enzyme.

The low-valent active forms of the Mn catalases have been demonstrated to have metal−metal distances several tenths of angstroms longer than that of the superoxidized enzyme. The low-resolution crystal structure, probably of the Mn^{III}_2 enzyme, gives a 3.6 Å Mn···Mn distance for the *T. thermophilus* catalase.[12,13] EXAFS analysis of the *L. plantarum* enzyme does not suggest that there is a short (<3.3 Å) distance for the isolated or reduced forms. Recently, EPR studies of the Mn^{II}_2 form of the *T. thermophilus* enzyme were analyzed to provide a Mn···Mn distance of 3.59 Å.[18] The core of the $Mn^{III/IV}$ enzyme has a 2.7 Å Mn···Mn distance and the strong coupling necessary to observe a 16 line EPR signal at 77 K.

While the Mn catalases have been studied for over 10 years, there are still few functional models for the low-valent catalytic cycle observed for the enzymes.[1,19−23] One approach we have taken is to use a ligand system that can support multiple oxidation states of a dinuclear manganese core, with minimal rearrangement of the ligand environment upon oxidation and reduction.[24]

The $[Mn(2\text{-}OHsalpn)]_2$ series of dinuclear complexes has been isolated and characterized crystallographically in all four oxidation states known for the Mn catalases (Mn^{II}_2, $Mn^{II/III}$, Mn^{III}_2, and $Mn^{III/IV}$).[24] In earlier studies, we[25−30] and others[31,32] also showed that asymmetric dimers containing the same ligand could be isolated and structurally characterized. Schematic diagrams of the symmetric and asymmetric dimers are provided in Figure 1. In this contribution, we use this dimer series to examine the catalytic activity of the Mn^{II}_2 and Mn^{III}_2 forms of this complex. We have previously shown that a symmetric Mn^{III}_2 dimer was the most active synthetic complex reported for hydrogen peroxide disproportionation chemistry.[1] The series of dimer derivatives presented in this work allows us to address the mechanism of peroxide binding and disproportionation[1] and to correlate the redox potential and ligand field contribution to the rate and efficiency of this catalytic process. Furthermore, this dimer system, which can be inactivated through the reaction of hydrogen peroxide with a mixed-valent intermediate, may provide mechanistic implications for the inactivation of the Mn catalases.

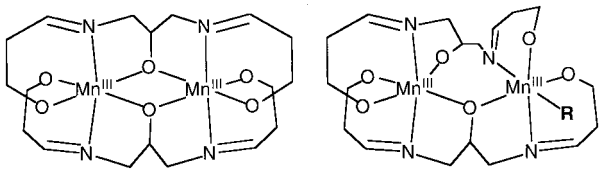

Figure 1. Schematic representation of the symmetric Mn^{III}_2 dimer (left) and the asymmetric Mn^{III}_2−solvento (right) complex.

Experimental Section

Materials. All solvents were HPLC grade, and no action was taken to remove excess water or to further purify the solvents (except where noted). Anhydrous hydrogen peroxide was prepared by a modification of a published procedure:[33] fifteen to twenty milliliters of a 50% hydrogen peroxide solution in water (Fisher) was placed in a 25-mL pear-shaped flask for micro-vacuum distillation. All glassware used in the procedure was soaked overnight in concentrated nitric acid and then washed with a 0.1 M EDTA solution for removal of trace metals. The peroxide solution was frozen in liquid nitrogen (LN_2) prior to distillation and then distilled at room temperature until the volume was reduced by two-thirds (approximately 4−5 h). Acetonitrile was added to the pure H_2O_2 to form a 2−10 M solution. *Caution: concentrated anhydrous hydrogen peroxide is potentially explosive and should be handled from behind a blast shield at all times.* This method produces >97% pure H_2O_2. The concentration of the peroxide stock solution was measured by titration of aqueous solutions with an aqueous $KMnO_4$ solution standardized against $Na_2S_2O_3$ (which had been standardized against potassium oxalate).

Deuterium peroxide (D_2O_2) was prepared by vacuum distilling 20 mL of 50% H_2O_2 to one-half of the volume, adding 10 mL of D_2O (99% D, atom, from Cambridge Isotope Labs), and redistilling to one-third of the volume. This was repeated two additional times to give a D_2O_2/H_2O_2 ratio of >93%. The D/H ratio was checked by Raman spectroscopy.

Isotopically labeled $H_2{}^{18}O_2$ was prepared by a modification of a published procedure:[34] 2-ethylanthraquinone (0.835 g, 3.54 mmol) was dissolved in 50 mL of a 50/50 benzene/decanol solvent mixture, and Pd/alumina (10 mg, 10 wt %) was added. The quinone was reduced under H_2 (3 atm) for 3 h. The fluorescent yellow-green hydroquinone solution was transferred under Ar to a 100-mL Schlenk-type flask leaving the Pd/alumina behind. A 100-mL flask equipped with a stopcock was filled with 1 atm (4.1 mmol) of $^{18}O_2$ (Isotec, 98% atom, ^{18}O). The flask was attached to the reaction vessel under Ar, and the stopcock was opened. The contents were washed through both flasks and stirred. The hydroquinone solution immediately became darker green. After 1 h, the mixture was again washed through both flasks. The solution had become lighter yellow after going through a brown intermediate. Stirring was continued for an additional1 h. The yellow solution was filtered to remove any additional Pd and extracted with 3 × 5 mL of cold water, yielding a 200 mM peroxide solution in water. The $^{18}O/^{16}O$ ratio (93%) was confirmed by Raman spectroscopy, through comparison of the areas of the peaks corresponding to the $^{18}O-{}^{18}O$ and $^{16}O-{}^{16}O$ stretches. The concentration of H_2O_2 was measured by titration with $KMnO_4$.

Complexes. The Mn^{II} and Mn^{III} dimers of 2-OH(X-sal)pn were prepared as described previously.[24] Solutions of the Mn^{II} dimers were prepared in degassed acetonitrile under Ar but were not protected from air during kinetic measurements. Solutions of the Mn^{III} dimers were prepared in acetonitrile under ambient conditions.

(17) Gamelin, D. R.; Kirk, M. L.; Stemmler, T. L.; Pal, S.; Armstrong, W. H.; Penner-Hahn, J. E.; Solomon, E. I. *J. Am. Chem. Soc.* **1994**, *116*, 2392−2399.
(18) Khangulov, S. V.; Pessiki, P. J.; Barynin, V. V.; Ash, D. E.; Dismukes, G. C. *Biochemistry* **1994**, *34*, 2015−2025.
(19) Mathur, P.; Crowder, M.; Dismukes, G. C. *J. Am. Chem. Soc.* **1987**, *109*, 5227−5233.
(20) Pessiki, P. J.; Dismukes, G. C. *J. Am. Chem. Soc.* **1994**, *116*, 898−903.
(21) Larson, E. J.; Pecoraro, V. L. *J. Am. Chem. Soc.* **1991**, *113*, 7809−7810.
(22) Bossek, U.; Saher, M.; Weyhermüller, T.; Wieghardt, K. *J. Chem. Soc., Chem. Commun.* **1992**.
(23) Sakiyama, H.; Okawa, H.; Isobe, R. *J. Chem. Soc., Chem. Commun.* **1993**, 882−884.
(24) Gelasco, A.; Kirk, M. L.; Kampf, J. W.; Pecoraro, V. L. *Inorg. Chem.* **1997**, *36*, 1829−1837.
(25) Bonadies, J. A.; Kirk, M. L.; Lah, M. S.; Kessissoglou, D. P.; Hatfield, W. E.; Pecoraro, V. L. *Inorg. Chem.* **1989**, *28*, 2037−2044.
(26) Bonadies, J. A.; Maroney, M. J.; Pecoraro, V. L. *Inorg. Chem.* **1989**, *28*, 2044−2051.
(27) Larson, E.; Haddy, A.; Kirk, M. L.; Sands, R. H.; Hatfield, W. E.; Pecoraro, V. L. *J. Am. Chem. Soc.* **1992**, *114*, 6263−6265.
(28) Caudle, M. T.; Riggs-Gelasco, P.; Gelasco, A. K.; Penner-Hahn, J. E.; Pecoraro, V. L. *Inorg. Chem.* **1996**, *35*, 3577−3584.
(29) Randall, D. E.; Gelasco, A.; Pecoraro, V. L.; Britt, R. D. *J. Am. Chem. Soc.* **1997**, *119*, 4481−4491.
(30) Caudle, M. T.; Pecoraro, V. L. *J. Am. Chem. Soc.* **1997**, *in press*.
(31) Bertoncello, K.; Fallon, G. D.; Murray, K. S.; Trekink, E. R. T. *Inorg. Chem.* **1991**, *30*, 3562−3568.
(32) Mikuriya, M.; Yamoto, T.; Tokii, T. *Bull. Chem. Soc. Jpn.* **1992**, *65*, 6−1468.
(33) Cofré, P.; Sawyer, D. T. *Inorg. Chem.* **1986**, *25*, 2089−2092.
(34) Sitter, A. J.; Terner, J. *J. Labelled Compd. Radiopharm.* **1984**, *22*, 461−465.

Methods. Solutions were prepared under Ar for ligand-exchange reactions and for gas chromatography−mass spectrometry (GC−MS) and EPR experiments. Solutions of H_2O_2 used in these experiments were prepared in degassed acetonitrile. H_2O_2 solutions for kinetic studies were prepared in dry acetonitrile and saturated with either Ar or dry air.

Initial Rate Measurements. Initial rate kinetic measurements on disproportionation of hydrogen peroxide by the synthetic catalysts were determined polarographically, using a Clark-type oxygen electrode. The electrode (Yellow Springs Instruments) was covered with a Teflon membrane held in place with Viton O-rings that are resistant to acetonitrile. The electrode was held at a potential of −0.8 V, and the rate of change of oxygen concentration was measured by observation of the current passed over time which is converted to V/s. Rate data were collected on a Zenith PC using a BASIC program previously described.[35] Air-saturated acetonitrile solutions were added to the cell, and the response of the electrode to dissolved O_2 was measured. The concentration of O_2 in air-saturated acetonitrile at 25 °C has been determined to be 2.43 mM.[36] Hydrogen peroxide solutions (1.7 mL) were added to the thermostated and stirred cell, data were collected for 15−20 s to establish a baseline, and then 100 μL of catalyst solution was added. The initial rate, mmol of H_2O_2/(s × mol of catalyst), was calculated by measuring the slope of the ΔV vs time curve obtained and by determining the rate of hydrogen peroxide disproportionation according to eq 2:

$$\text{rate } (s^{-1}) = \frac{\text{slope (V/s)}\dfrac{2.43\ (\text{mM } [O_2])}{\Delta V(\text{air satd } CH_3CN)}\dfrac{2H_2O_2}{1O_2}\,1.8\ \text{mL}}{n\ (\text{mol of catalyst})} \qquad (2)$$

The response of the electrode was measured periodically during experimental runs, and calculations were made accordingly.

UV−visible spectra were measured on a Perkin-Elmer lambda 9 dual beam scanning spectrophotometer, with scan rates from 240 to 960 nm/min. Additional spectroscopic data were acquired on an OLIS-RSM stopped-flow spectrometer at a scan rate of 1−10 full spectrum scans/s. X-band electron paramagnetic resonance (EPR) spectra were collected with a Brüker ER-200-SRC spectrometer with a modified console with TM(110) cavity. Spectra were measured at 77 K using a liquid nitrogen finger Dewar cavity insert. Typical parameters were as follows: frequency, 9.445 GHz; peak-to-peak modulation, 5 G; modulation frequency, 100 kHz; power, 20.2 mW. Samples for monitoring catalase reactions were flash frozen in LN_2 after the addition of the reactants. Fast atom bombardment mass spectrometry (FAB-MS) measurements were conducted at the Chemistry Department Mass Spectrometry Facility at The University of Michigan. Samples were prepared as described below, and solids were isolated and stored under Ar; spectra were collected using a 3-nitrobenzyl alcohol matrix.

Results

Catalase Activity. The symmetric Mn^{III} dimer $[Mn^{III}(2\text{-}OHsalpn)]_2$ is the air stable form of this series of manganese complexes[24] and reacts in acetonitrile with excess hydrogen peroxide to evolve oxygen and water.[1] This symmetric dimer reacts catalytically and is stable for thousands of turnovers in acetonitrile. The addition of excess H_2O_2 (>10-fold) to a solution of $[Mn^{III}(2\text{-}OHsalpn)]_2$ or $[Mn^{III}(2\text{-}OH(3,5\text{-}Clsal)pn)]$ in acetonitrile shows no time-dependent change in the UV−visible spectrum. However, the addition of 1−4 equiv of hydrogen peroxide to a 50:50 acetonitrile/DMF solution of $[Mn^{III}(2\text{-}OH(3,5\text{-}Clsal)pn)]_2$ shows a shift in the UV−visible spectrum to higher energy consistent with that of the Mn^{II} dimer $[Mn^{II}(2\text{-}OH(3,5\text{-}Clsal)pn)]_2^{2-}$. A series of time-dependent electronic spectra from 0 to 4 min of the 50:50 acetonitrile/DMF solution of $[Mn^{III}(2\text{-}OH(3,5\text{-}Clsal)pn)]_2$ reacting with 2 equiv of hydrogen peroxide is shown in Supporting Information Figure S1-A. Supporting Information Figure S1-B shows a series of spectra from 4 to 30 min showing the reoxidation to the Mn^{III} starting complex by molecular oxygen. The oxidation of the Mn^{II} dimers is slow, relative to the time frame of the kinetics runs with hydrogen peroxide. No correction was made for the oxidation in the following kinetics experiments, since less than 1% of the Mn^{II} dimer is oxidized by ambient O_2 during the typical run.

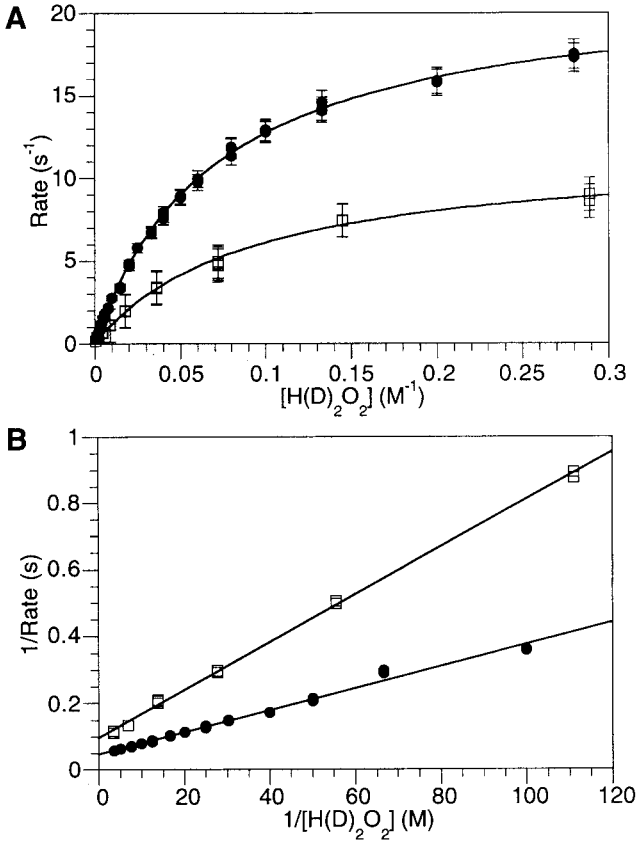

Figure 2. (A) Rate of hydrogen (deuterium) peroxide disproportionation vs $[H(D)_2O_2]$. Catalyst = $[Mn^{III}(2\text{-}OH(5\text{-}Clsal)pn)]_2$, 11 μM (20 nmol/run). Closed circles, hydrogen peroxide; open squares, deuterium peroxide. Best fit lines gives the kinetic parameters $k_{cat} = 21.9 \pm 0.2$ s^{-1} and $K_M = 72 \pm 1$ mM for H_2O_2 and $k_{cat} = 11.6 \pm 0.3$ s^{-1} and $K_M = 91 \pm 5$ mM for D_2O_2. (B) Lineweaver−Burke representation of data in A showing the isotope effect through the different slopes representing k_{cat}/K_M for each substrate.

The initial rates of oxygen production for the disproportionation reactions in acetonitrile were measured under pseudo-first-order conditions of hydrogen peroxide concentrations. Both the oxidized (Mn^{III}_2) and reduced (Mn^{II}_2) forms of the $[Mn(2\text{-}OH\text{-}(5\text{-}Clsal)pn)]_2$ dimers exhibit substrate saturation kinetics with excess hydrogen peroxide.[1] Figure 2 shows the plot of the replicate data sets of the initial rate of H_2O_2 consumption vs the substrate concentration at a constant catalyst concentration for $[Mn^{III}(2\text{-}OH(5\text{-}Clsal)pn)]_2$. The data were fit to the Michaelis−Menten equation by using KaleidaGraph 3.0 for the Macintosh, and the catalytic turnover number ($k_{cat} = 21.9 \pm 0.2$ s^{-1}) and the Michaelis constant ($K_M = 72 \pm 1$ mM) were determined.

This is the first example of a synthetic dimeric model for the Mn catalases that shows Michaelis−Menten behavior, usually observed for enzyme systems.[1] Substrate saturation behavior implies a rapid equilibrium between unbound substrate and a catalyst−substrate complex. Under conditions of high (saturat-

(35) Stemmler, T. J., Ph.D. Thesis, University of Michigan, 1996.
(36) Franco, C.; Olmstead, J., III *Talanta* **1990**, *37*.

Table 1. Kinetic Parameters[a] for the Ring-Substituted Mn^{III} Dimers

derivative	k_{cat} (s^{-1})	K_M (mM)	k_{cat}/K_M ($s^{-1}\cdot M^{-1}$)	est $E_{1/2}$ ($III_2 \leftrightarrow II_2$), mV[c]
$[Mn^{III}$(2-OH(5-MeOsal)pn)$]_2$	4.2 ± 0.1	11.0 ± 2	382 ± 80	−618
$[Mn^{III}$(2-OHsalpn)$]_2$	10.1 ± 0.2	10.2 ± 0.4	990 ± 60	−500
$[Mn^{III}$(2-OH(5-Clsal)pn)$]_2$	21.9 ± 0.2	72.0 ± 1	305 ± 7	−400
$Na_2[Mn^{II}$(2-OH(5-Clsal)pn)$]_2$[b]	20.8 ± 0.8	68.0 ± 4	308 ± 30	−400
$[Mn^{III}$(2-OH(3,5-Clsal)pn)$]_2$	18.6 ± 0.5	118.0 ± 6	160 ± 13	−270

[a] Based on fits of the Michaelis−Menten equation to the rate data shown in Figure 3. [b] The Mn^{II} dimer of 2-OH(5-Clsal)pn was also examined for saturation kinetics to show the independence of the initial oxidation level. The shape of the curve is indistinguishable from that of $[Mn^{III}$(2-OH(5-Clsal)pn)$]_2$ shown in Figure 2A. [c] Estimated $III_2 \leftrightarrow II_2$ potentials(vs SCE) are taken from Table 3 in ref 24.

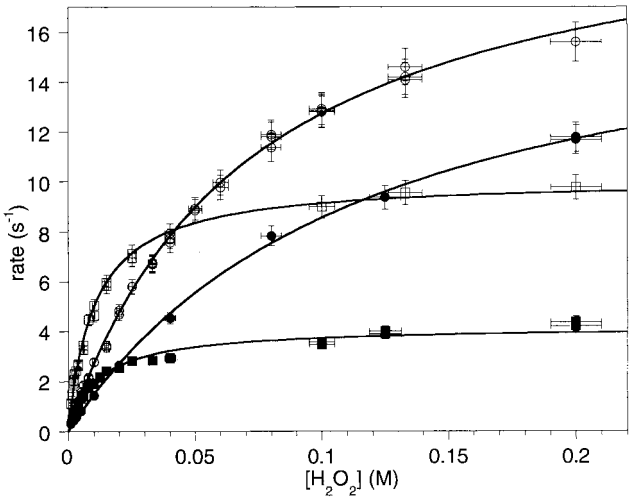

Figure 3. Rate of H_2O_2 disproportionation vs $[H_2O_2]$ for the different ring-substituted Mn^{III} dimers. [Catalyst] = 11 μM (20 nmol/run). Legend: (○) 5-Cl, (●) 3,5-Cl, (□) 5-H, (■) 5-MeO. Kinetic parameters for each dimer are contained in Table 1.

ing) substrate concentration, the primary species in solution is the catalyst−substrate complex. The rate of the reaction is then dependent only on the decomposition of the catalyst−substrate complex to the product and the free catalyst.

The same experiments were run using a series of ring-substituted derivatives of $[Mn^{III}$(2-OHsalpn)$]_2$. The results of these runs are summarized in Table 1. The data for these derivatives and the fits to the data are shown in Figure 3. The 5-Cl derivative proved to be the most active and was used for further kinetic and isotope experiments. The best fit curves shown in Figure 3 are qualitatively different in simple saturation behavior from one another and from previously reported results. The shapes of the curves allow mechanistic data to be extracted directly from qualitative analysis of the data. Two distinct saturation curves are observed for this series. A low K_M value is found for both of the electron-releasing ligand derivatives, 2-OH(5-MeOsal)pn and 2-OHsalpn, which may stabilize the Mn(III) dimer. The electron-withdrawing ring derivatives, 2-OH(5-Clsal)pn and 2-OH(3, 5-diClsal)pn, have saturation curves representative of the high K_M values, indicating that these complexes are less efficient at binding the hydrogen peroxide substrate.

The order of the reaction was determined by examining the initial rates at nonsaturating levels of peroxide. At low substrate concentrations, the reaction is first order in peroxide concentration as shown in Figure 4A. The slope of the line provides the bimolecular rate constant for a second-order reaction of 300 $s^{-1}\cdot M^{-1}$.

The molecularity of the reaction with respect to the catalyst concentration was measured by varying the Mn dimer concentration at a constant peroxide concentration. As predicted from the observed saturation kinetics, at high substrate concentrations,

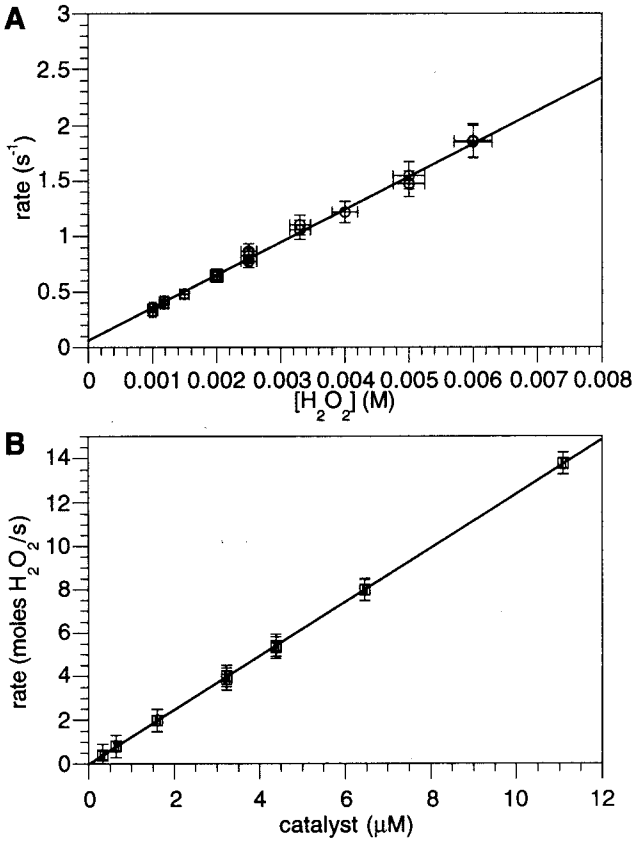

Figure 4. (A) Rate vs $[H_2O_2]$ at low peroxide concentrations. Catalyst = $[Mn^{III}$(2-OH(5-Clsal)pn$)]_2$; catalyst concentration = 11 μM (20 nmol/run). Slope = 300 ± 20 $s^{-1}\cdot M^{-1}$. (B) Rate (mol of $H_2O_2^{-1}$) vs [catalyst]. Catalyst = $[Mn^{III}$(2-OH(5-Clsal)pn$)]_2$; hydrogen peroxide concentration = 100 mM. Slope = 12.4 ± 0.8 s^{-1} mol of H_2O_2/mol of catalyst.

the reaction rate should be dependent only on the catalyst concentration. Figure 4B shows the plot of rate of disproportionation of hydrogen peroxide in mol of H_2O_2/s versus catalyst concentration. The concentration of hydrogen peroxide was 100 mM. The linear dependence of the rate with respect to the catalyst concentration confirms the first-order dependence on the catalyst, and the observed first-order rate constant for the catalyst dependence can be extracted from the slope of the line under these conditions of initial rate measurements. The rate equation that is consistent with the observed kinetic data at low $[H_2O_2]$ is shown in eq 3.

$$\text{rate} = k[\text{cat}]^1[H_2O_2]^1 \quad (3)$$

Deuterium Isotope Studies. Using isotopically labeled hydrogen peroxide, we were able to observe a deuterium isotope effect on the disproportionation reaction and to examine the mechanism of oxygen formation. The reaction of $[Mn^{III}$(2-OH(5-Clsal)pn$)]_2$ with excess D_2O_2 exhibits substrate saturation kinetics as was observed with H_2O_2. Figure 2A shows the plot

of the rate of D_2O_2 disproportionation versus the concentration of deuterium peroxide. The replicate sets of data were fit to the Michaelis−Menten equation, and the kinetic parameters k_{cat} ($11.6 \pm 0.3\ s^{-1}$) and K_M (91 ± 5 mM) were determined. The Lineweaver−Burke plot of these data is shown in Figure 2B. The slope of the linear fit to these data gives a k_{cat}/K_M value that compares well to that obtained from the fit to the raw initial rate data (140 vs 130 $s^{-1}\cdot M^{-1}$). On the basis of these results, it is clear that the turnover-limiting step of this reaction has a proton dependence. Comparison of the catalytic efficiency, k_{cat}/K_M, for the H_2O_2 vs the D_2O_2 reactions gives a deuterium isotope effect of $K_H/K_D = 2.2$. While it is clear from this analysis that there is a proton-dependent step, whether this is an actual kinetic isotope effect or an equilibrium effect (pK_a variation) has not been determined.

Catalyst Structure. Reaction of excess hydrogen peroxide with a mixture of $Na_2[Mn^{II}(2\text{-}OHsalpn)]_2$ and $Na_2[Mn^{II}(2\text{-}OH(5\text{-}NO_2sal)pn)]_2$ in acetonitrile converts the complexes to their Mn^{III} derivatives. The negative ion FAB-MS of the mixture of the two Mn^{II} complexes contains peaks that correspond only to the parent compounds (Figure S2). This spectrum confirms that the dimers do not exchange ligands in the time course of the disproportionation reaction (approximately 5 min). The positive ion FAB-MS of the solid isolated after reaction of the mixture of the catalysts with 100 equiv of H_2O_2 shows only conversion to the Mn^{III} derivatives with no peaks in the mass spectrum indicative of ligand exchange ($[Mn^{III}_2(2\text{-}OH(5\text{-}NO_2sal)pn)(2\text{-}OHsalpn)]$), Figure S3. The mixed-ligand derivatives were prepared synthetically, and the negative ion FAB-MS shows that the mixed-ligand derivatives can be observed when formed.

The oxidation state of the active catalyst was probed by EPR spectroscopy of the catalyst during reaction with hydrogen peroxide. Addition of 10 equiv of H_2O_2 to a vented acetonitrile solution of $Na_2[Mn^{II}(2\text{-}OHsalpn)]_2$ caused a rapid loss of the Mn^{II}_2 EPR signal. There was no EPR signal for the product of the peroxide reaction. This is due, presumably, to the presence of a Mn^{III}_2 dimer only, since the other oxidation states for this dimer system (Mn^{II}_2, $Mn^{II/III}$, and $Mn^{III/IV}$) are EPR active.[24] This is consistent with the FAB-MS experiments and UV−visible spectroscopy. Only in the case where $Na_2[Mn^{II}(2\text{-}OH(5\text{-}NO_2sal)pn)]_2$ was used as the catalyst was an EPR signal observed. For this dimer, a diminished Mn^{II}_2 EPR signal was observed; this is probably due to the slow oxidation of the $[Mn^{II}(2\text{-}OH(5\text{-}NO_2sal)pn)]_2^{2-}$ complex to the Mn^{III} dimer by O_2 or peroxide. It has been observed for this system that the Mn^{II}_2 species is first oxidized to a $Mn^{II/III}$ dimer by air, and then the $Mn^{II/III}$ dimer is slowly converted to the Mn^{III}_2 complex.[24]

Inactivation. The addition of 60 equiv of H_2O_2 to an EPR tube containing 0.5 mL of a 5 mM DMF solution of $Na_2[Mn^{II}(2\text{-}OH(5\text{-}NO_2sal)pn)]_2$ generated a new species which, at 77 K, has a 16 line EPR spectrum. This new spectrum is remarkably similar to that observed for the inactive "superoxidized" Mn catalase[10] and was very different from the EPR spectrum for the dialkoxide-bridged $[Mn^{III/IV}(2\text{-}OHsalpn)_2]^+$ dimer previously described.[24] The new spectrum is identical to that observed in Figure 5E and is most similar to that for the dioxo-bridged $Mn^{III/IV}$ dimer $[Mn(salpn)(O)]_2^-$,[37] the one-electron-reduced derivative of $[Mn^{IV}(salpn)(O)]_2$.[38]

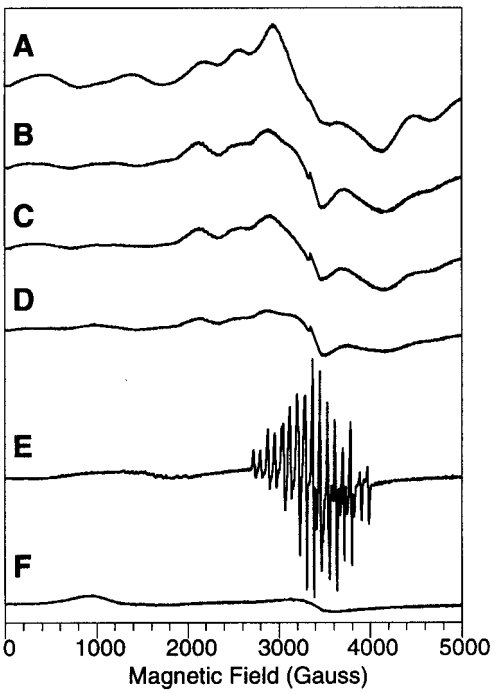

Figure 5. Reaction of $[Mn^{II}_2(2\text{-}OH(5\text{-}NO_2sal)pn)_2]^{2-}$ dimer in DMF with varying quantities of H_2O_2 in a closed EPR tube. The bottom spectrum shows the effect of O_2 on the Mn^{II} dimer—conversion to the $Mn^{II/III}$ dimer.

The formation of this mixed-valent "dioxo" species was studied by following this reaction under more stoichiometric peroxide conditions. Figure 5 shows the effect on the EPR spectrum of $Na_2[Mn^{II}(2\text{-}OH(5\text{-}NO_2sal)pn)]_2$ as varying amounts of hydrogen peroxide were added to the EPR tube. When 1, 2, or 4 equiv of H_2O_2 was added, the Mn^{II}_2 signal was diminished. When 40 equiv was added, the spectrum converted to the 16 line signal. The final spectrum shows the effect on the Mn^{II}_2 signal by bubbling O_2 through a chilled solution for 2 min. This signal is that of the dialkoxide-bridged $Mn^{II/III}$ dimer.[24]

Since this dioxo $Mn^{III/IV}$ dimer was only observed under conditions of high O_2 concentration and oxidation of $[Mn^{II}(2\text{-}OH(5\text{-}NO_2sal)pn)]_22-$ by oxygen had been shown to form the dialkoxide $Mn^{II/III}$ dimer, the effect of H_2O_2 on the EPR spectrum of the $Mn^{II/III}$ dimer was examined. Upon addition of as little as 1 equiv of H_2O_2 to a solution of $[Mn^{II/III}(2\text{-}OH(5\text{-}NO_2sal)pn)_2]^-$, the EPR spectrum is converted to the 16 line signal.

Solutions of the $Mn^{III/IV}$ dimer were not competent for the H_2O_2 disproportionation reaction. For conditions where the rate measured for the Mn^{II}_2 dimer was $8.5\ s^{-1}$, the rate measured for the solution of the 16 line species (assuming >90% conversion) was $<0.2\ s^{-1}$. For solutions taken from the reaction of the Mn^{II}_2 dimer with H_2O_2 under vented conditions (where only Mn^{III}_2 is formed), the rate measured was $7.2\ s^{-1}$. Therefore, the formation of this "dioxo-bridged" $Mn^{III/IV}$ dimer is a pathway for inactivation of this low-valent catalyst system.

Discussion

The $[Mn(2\text{-}OHsalpn)]_2$ system is the only catalase mimic that has been isolated and characterized crystallographically in both the oxidized and reduced forms of the catalyst. Prior to this work, only one synthetic dimer that was a functional mimic for the low-valent catalytic cycle of the Mn catalases had been prepared.[19,20] Only recently has this complex been characterized

(37) Horwitz, C. P.; Winslow, P. J.; Warden, J. T.; Lisek, C. A. *Inorg. Chem.* **1993**, *32*, 82−88.
(38) Larson, E. J.; Pecoraro, V. L. *J. Am. Chem. Soc.* **1991**, *113*, 3810−3818.

Table 2. Kinetic Parameters of Reported H_2O_2 Disproportionation Catalysts

catalyst[a]	rate (s^{-1})	k_{cat}/K_M ($M^{-1}\cdot s^{-1}$)	Mn redox cycle	Mn−Mn distance (Å)	ref
Mn catalase[b]	200000	570000	III/III ↔ II/II	3.6 (Mn^{II}_2)[c]	7, 13
$[Mn^{IV}(salpn)O]_2$	250	1000	IV/IV ↔ III/III	2.73	21, 43
$[Mn^{III}(2\text{-}OH(X\text{-}sal)pn)]_2$/ $[Mn^{II}(2\text{-}OH(X\text{-}sal)pn)]_2^{2-}$	22 (4−22) range	350 (70−420) range	III/III ↔ II/II	3.247 (Mn^{III}_2) 3.332 (Mn^{II}_2)	1, tw
$[Mn^{II}(2\text{-}OHpicpn)]_4(ClO_4)_4$	150	70	(II_4 ↔ II_2III_2)	3.72 (average)	37
$[Mn^{III/IV}(L^1)(O)_2(OAc)(bpy)(MeOH)(ClO_4)_2$	13.2	b	(III/IV ↔ II/III)	2.630	22
$[Mn^{III/IV}(L^1)(O)_2(\mu\text{-}OAc)(OAc)_2]$	5.5	b	(III/IV ↔ II/III)	2.665	22
$[Mn^{III}_2(anthracenediporphyrin)]Cl_2$	5.4	b	IV/IV ↔ III/III	4.5 (Mn^{III}_2)	48
$[Mn^{II}_2(L^2)(\mu\text{-}OAc)(BuOH)](ClO_4)_2$	1.2	b	III/III ↔ II/II	3.540	19, 20
$(Ba,Ca)_2[Mn_4(\mu\text{-}O)(\mu\text{-}OH)(OAc)_2(L^3)_2]$	1.04	b	N/A	3.38, 3.58, 3.72	c
$[Mn^{II}_2(L^4)(\mu\text{-}C_6H_5CO_2)_2(NCS)]$	0.79	b	IV/IV ↔ III/III or II/III ↔ II/IV	3.325	23
$[Mn^{III/IV}(dpa)_2(O)_2]ClO_4$	0.26	b	(III/IV ↔ II/III)	2.656	d
$[Mn^{III}(TPP)]^-$	0.013	b	(V ↔ III)		48
$[Mn^{II}(H_2O)_6](ClO_4)_2$	0.0063	b	unknown		tw

[a] L^1 = 1,4,7-trimethyl-1,4,7-triazacyclononane; L^2 = *N*,*N*,*N*′,N′-tetrakis(2-methylene-benzimidazolyl)-1,3-diaminopropan-2-ol; L^3 = *N*,*N*,*N*′,N′-tetraacetate-1,3-diaminopropan-2-ol; L^4 = 2,6-bis(*N*-(2-(dimethylamino)-ethyl)iminomethyl)-4-methylphenolate; bpy = 2,2′-bipyridine; Hdpa = *N*,*N*-bis(2-pyridylmethyl)glycine; TPP = tetraphenylporphrin. tw = this work. [b] Saturation kinetics not reported. [c] Nishida, Y.; Akamatsu, T.; Tsuchiya, K.; Sakamoto, M. *Polyhedron* **1994**, *13*, 2251−2254. [d] Stibrany, R. T.; Gorun, S. M. *Angew. Chem., Int. Ed. Engl.* **1990**, *29*, 1156−1158.

Scheme 1

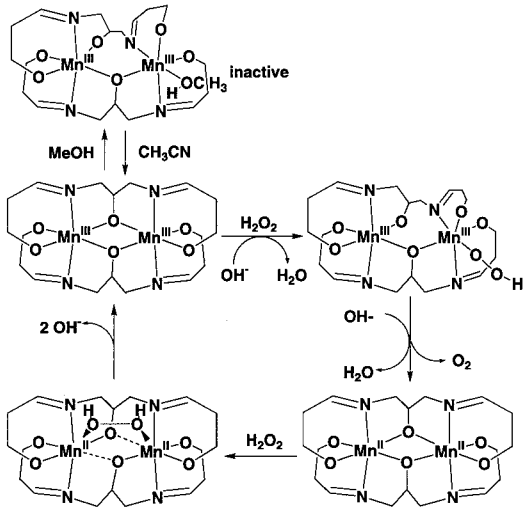

crystallographically[39] and in only the Mn^{II}_2 oxidation state. Table 2 compiles the known synthetic catalase mimics, with their kinetic, redox, and structural parameters. The most active manganese-containing hydrogen peroxide disproportionation catalyst reported to date is $[Mn^{IV}(salpn)(\mu_2\text{-}O)]_2$. This complex is thought to be an excellent model for the alternate catalase reactions of the oxygen-evolving complex; however, the operable oxidation levels ($Mn(IV)_2$ to 2 Mn(III)) do not match those of the manganese catalase. The other system that has k_{cat} in excess of the $[Mn(2\text{-}OHsalpn)]_2$ system is a tetranuclear assembly which requires all four manganese atoms for the reaction. If one uses k_{cat}/K_M as a measure of enzymatic efficiency, then the $[Mn(2\text{-}OHsalpn)]_2$ system is within a factor of 2000 of enzymatic catalysis.[40] All other compounds are inferior as catalase mimics using the criteria of rates and the lack of reported substrate saturation behavior.

Mechanism of Catalase Activity. The $[Mn(2\text{-}OHsalpn)]_2$ system cycles between the Mn^{II}_2 and Mn^{III}_2 oxidation levels while disproportionating hydrogen peroxide. Scheme 1 shows a mechanism for the catalytic disproportionation of hydrogen peroxide by the $[Mn(2\text{-}OHsalpn)]_2^{2-/0}$ dimers which is consistent with the observed results of this study.

That the first step upon reaction of H_2O_2 with the Mn^{III}_2 dimer is a reduction to form the Mn^{II}_2 species with concomitant evolution of oxygen was shown by the use of ring-substituted derivatives that are more difficult to oxidize to the Mn^{III}_2 dimer. While the reaction of $[Mn^{III}(2\text{-}OHsalpn)]_2$ with H_2O_2 proceeds vigorously without a spectroscopic change, $[Mn^{III}(2\text{-}OH(3,5\text{-}Clsal)pn)]_2$ shows an immediate shift in the UV−visible spectrum which is consistent with the accumulation of the Mn^{II} dimer $[Mn^{II}(2\text{-}OH(3,5\text{-}Clsal)pn)]_2^{2-}$. Additional support for the initial reduction comes from the inability of the other related dimers in this series ($[Mn^{II/III}(2\text{-}OHsalpn)]_2^-$, $[Mn^{III/IV}(2\text{-}OHsalpn)]_2^+$, $\{[Mn^{IV/IV}(2\text{-}OHsalpn)]_2OH\}^+$, and $[Mn^{IV}(2\text{-}OHsalpn)(\mu_2\text{-}O)]_2$) to carry out peroxide disproportionation.[41] Interestingly, we have shown that the reaction of *tert*-butylhydroperoxide with $[Mn^{III}(2\text{-}OHsalpn)]_2$ results in the initial oxidation of the dimer to form $\{[Mn^{III/IV}(2\text{-}OHsalpn)]_2OH\}$.[28]

Both mass spectrometry and EPR experiments have shown that these dimers do not decompose into monomeric compounds during the catalytic cycle. This is further supported by the first-order dependence of the reaction rate on catalyst concentration. Thus, the low-valent and high-valent intermediates that are formed must also maintain their dinuclear integrity. The two-electron oxidation of the dinuclear center can be accommodated with very little ligand rearrangement, as shown by the crystal structures of the oxidized and reduced forms of the catalyst.[24] The Mn−Mn distance changes by only 0.1 Å between the Mn^{II}_2 and the Mn^{III}_2 oxidation states. More importantly, the 2-OHsalpn ligand set maintains the general geometry around the Mn ions over the whole range of oxidation states. Upon oxidation, there are only slight angular rearrangements of the ligand environment.[24] The dinuclear core facilitates the disproportionation reaction by providing two redox-active centers in close proximity that are each capable of one-electron chemistry.

Because we have been able to isolate and characterize the $[Mn(2\text{-}OH(X\text{-}sal)pn)]_2$ complexes over four oxidation levels, we can use EPR spectroscopy to establish which Mn species are present under different solution conditions. The EPR experiments showing rapid loss of the Mn^{II}_2 signal upon reaction with excess hydrogen peroxide indicate that the Mn^{III}_2 form of the catalyst is the primary species in solution since all other known forms of the Mn dimers are EPR active. This result,

(39) Pessiki, P. J.; Khangulov, S. V.; Ho, D. M.; Dismukes, G. C. *J. Am. Chem. Soc.* **1994**, *116*, 891−897.

(40) This comparison is between the maximal rate of the *L. plantarum* enzyme in water at pH 7.2 and that of the $[Mn(2\text{-}OHsalpn)]_2$ system in acetonitrile.

(41) Gelasco, A.; Caudle, M. T.; Pecoraro, V. L., unpublished results.

combined with the lack of significant change in the electronic spectrum of the $[Mn^{III}(2\text{-}OHsalpn)]_2$ dimer upon reaction with excess peroxide, indicates that the slow step of this cycle is probably the oxidation of hydrogen peroxide with the concomitant reduction of the catalyst to the $Mn^{II}{}_2$ dimer. This step is presumably the turnover-limiting step, and the lack of observation of any significant $Mn^{II}{}_2$ levels indicates that the ratio of the rate-limiting step to the faster rates is rather high.

The observation of substrate saturation kinetics for $[Mn(2\text{-}OH(X\text{-}sal)pn)]_2$ indicates that a catalyst−peroxide intermediate must exist in the cycle; however, the kinetics alone do not distinguish at which point this intermediate forms. As we assign the initial dimer *reduction* as the turnover-limiting step, we must be able to account for the observed substrate saturation behavior at this step. One of the intriguing features of the $[Mn(2\text{-}OHsalpn)]_2$ compounds is their ability to participate in an alkoxide shift[25−29,31] that is reminiscent of carboxylate shifts in model compounds and proteins.[42−44] Figure 1 shows schematically the minimal ligand rotation that occurs upon attack at one Mn ion by methanol, THF, or, presumably, hydrogen peroxide. This alkoxide shift makes possible a coordination site for the substrate. Furthermore, the binding of methanol, THF, water, or hydroxide to $[Mn^{III}(2\text{-}OHsalpn)]_2$ or $[Mn^{III/IV}(2\text{-}OHsalpn)_2]^+$ does not significantly perturb the UV−visible spectra of the compounds. We have seen that the affinity for these small molecules follows the trend $Mn^{III}Mn^{IV} > Mn^{III}{}_2 \gg Mn^{II}Mn^{III} \gg Mn^{II}{}_2$.[30] These thermodynamic affinities underscore the likelihood that it is the Mn^{III} dimer that undergoes an alkoxide shift to bind H_2O_2, leading to the observed saturation behavior without direct spectroscopic observation of an intermediate.

During the course of this work, a $Mn^{III}{}_2$ dimer using a similar ligand to 2-OHsalpn, salmp, was prepared and characterized crystallographically by Holm and co-workers.[45] This ligand, which has three phenolate moieties, forms similar pentachelated dimeric Mn complexes containing a diphenolate-bridged Mn_2 core. The redox potentials and structural features of this dimer series are similar to those observed for the $[Mn(2\text{-}OHsalpn)]_2{}^{2-,1-,0}$ series;[24] therefore, we examined $[Mn^{III}(salmp)]_2$ for catalase activity. The $[Mn^{III}(salmp)]_2$ complex was completely inactive under all conditions examined and, in particular, under conditions in which $[Mn(2\text{-}OHsalpn)]_2$ is a very efficient catalase mimic. This apparent disparity may be caused by the inability of $[Mn^{III}(salmp)]_2$ to form the asymmetric end-on peroxide complex proposed in the mechanism of $[Mn(2\text{-}OHsalpn)]_2$. The salmp ligand system has a more rigid backbone that may preclude a "phenoxide shift" preventing the reaction with hydrogen peroxide.

Assuming that the first step of the reaction is binding hydrogen peroxide to form a ternary $\{[Mn^{III}(2\text{-}OH(salpn))]_2\text{-}(H_2O_2)\}$ complex, one must address how peroxide is oxidized to form dioxygen. Preparation of ^{18}O-labeled hydrogen peroxide in over 90% $^{18}O_2$ purity has allowed us to examine the source of the evolved oxygen.[1,46] The GC-MS of the head gas formed from the disproportionation of a 50:50 $H_2{}^{18}O_2/H_2{}^{16}O_2$ solution in acetonitrile by $[Mn^{III}(2\text{-}OH(5\text{-}Clsal)pn)]_2$ shows only peaks for $^{18}O_2$ ($m/e = 36$) and $^{16}O_2$ ($m/e = 32$), with no evidence for $^{18}O^{16}O$ ($m/e = 34$) formation. This result is consistent with that observed for the *L. plantarum* Mn catalase,[47] indicating that there is no O−O bond cleavage during the oxidation of hydrogen peroxide by these catalysts. This observation rules out the intermediacy of high-valent Mn=O species in the O_2-forming step.

There are catalase mimics that cleave the O−O bond during peroxide oxidation. This usually is indicative of a Mn=O intermediate with two examples of this type reported for manganese chemistry. Sakiyama and co-workers[23] prepared a Mn^{II} dimer with a phenolate−dicarboxylate bridging core that, upon reaction with hydrogen peroxide, is reported to form an intermediate containing either a $Mn^{II}Mn^{IV}$=O or $Mn^{IV}Mn^{IV}$=O core, as suggested by FAB-MS. Naruta and co-workers[48] observed that manganese(III)−porphyrin (MnP) complexes linked by rigid spacers disproportionated H_2O_2 and scrambled the $^{18}O_2$ label, thus presuming $Mn^{IV}P$=O intermediates which could combine to produce O_2. $[Mn^{III}(2\text{-}OHsalpn)]_2$ is initially reduced by peroxide which eliminates a higher-valent oxo species as a precursor to dioxygen production. This observation predicts that peroxide oxidation should occur in a two-electron step that does not scramble oxygen labels in the substrate.

While protons are among the most important factors that moderate reaction rates, conclusively establishing protonation states of catalyst or substrates can be a daunting task. In an effort to address this question, we carried out kinetics studies using D_2O_2 as substrate. The observation of a deuterium isotope effect in both k_{cat} and K_M underscores the important role protons play in this system. The effect on K_M is relatively small; $K_M(H)/K_M(D) = 0.78$ but is significant to the overall efficiency of the catalyst. Since K_M is related to the formation of the substrate−catalyst complex, an increase in K_M is consistent with a proton-dependent step being involved with substrate binding. Effectively, the increase in K_M for this system is indicative of poorer substrate binding; that is, it is more difficult for the catalyst to reach maximum efficiency. The deuterium isotope effect observed may be an equilibrium effect, with the pK_a of the deuterium peroxide being higher than that for hydrogen peroxide, or it could be related to concurrent protonation of a dimer position such as that of the alkoxide involved in the alkoxide shift. Unfortunately, the interpretation of isotope effects for substrates with readily dissociable protons is far more difficult than for systems containing C−H bonds. Thus, while we cannot further identify the role of protons in this process, it is clear that they are important ;otherwise, only a k_{cat} perturbation would be observed.

A larger deuterium isotope effect is observed for k_{cat}. The maximal rate for the disproportionation reaction is decreased by nearly one-half, with $k_{cat}(H)/k_{cat}(D) = 1.9$, corresponding to an overall $K(H)/K(D)$ ratio of 2.4. This effect is directly related to the rate-limiting step and is consistent with the concurrent loss of protons upon oxidation of hydrogen peroxide. Whether deprotonation and oxidation are simultaneous processes or oxidation is triggered by removal of a proton cannot be addressed at this point.

We have examined the kinetics profiles for the range of phenyl-ring substituted derivatives which vary in their reduction potentials and affinities for binding small molecules. The data presented in Figure 3 and Table 1 illustrate that all of the complexes show saturation kinetics; however their behavior can be organized into two groups on the basis of k_{cat} and K_M values. The more electron-donating ligands (5-MeO and 5-H) have low turnover numbers but appear to bind the peroxide very well

(42) Feig, A. L.; Lippard, S. J. *Chem. Rev.* **1994**, *94*, 759−805.
(43) Rosenzweig, A. C.; Frederick, C. A.; Lippard, S. J.; Nordlund, P. *Nature* **1993**, *366*, 537−543.
(44) Rosenweig, A.; Takahara, P. M.; Lippard, S. J. *Chem. Biol.* **1995**.
(45) Yu, S.-B.; Wang, C.-P.; Day, E. P.; Holm, R. H. *Inorg. Chem.* **1991**, *30*, 4067−4074.
(46) Gelasco, A.; Askenas, A.; Pecoraro, V. L. *Inorg. Chem.* **1996**, *35*, 1419−1420.
(47) Waldo, G. S., Ph.D. Thesis, University of Michigan, 1992.
(48) Naruta, Y.; Maruyama, K. *J. Am. Chem. Soc.* **1991**, *113*, 3595−3596.

with similar K_M values (11.0 and 10.2 mM). This is consistent with a slow turnover-limiting step (peroxide oxidation) due to the relative stabilization of the Mn^{III} oxidation state for the 5-MeO and 5-H dimers. In contrast, the electron-poor ligand derivatives (5-Cl and 3,5-Cl) have higher maximal rates than the 5-MeO and 5-H dimers but have much worse binding constants for peroxide (K_M). The higher rates observed for the electron-withdrawing ligand derivatives reflect the greater oxidizing power of these compounds which facilitates peroxide oxidation leading to enhanced maximal rates. If K_M is considered as a K_d for the formation of the Mn^{III}−peroxide complex, then the trend observed for K_M in this series can be related to the affinity of peroxide for the complex. Peroxide binding may be dependent on the alkoxide shift which converts the bisalkoxide-bridged dimers to the asymmetric, terminal peroxide complex, a model which has been observed with the solvent-bound dimer shown in Figure 1. One would expect that the strength of the Mn−alkoxide bond is dependent on the donor ability of the phenolate oxygens. The stronger the donation from the phenolates, the weaker will be the interaction between the manganese and the alkoxides which in turn reflects the tendency for the complex to engage in an alkoxide shift. Electron-donating derivatives can easily undergo the alkoxide shift and bind small molecules readily (lower K_M), while the more electron-withdrawing ligand derivatives would be expected to have higher K_M values.

The shape of the two different sets of curves shows immediately how different the catalytic efficiency is between the two types of dimers. Electron-donating derivatives bind peroxide well but are less able to carry out peroxide oxidation. These derivatives are easily saturated but never attain high maximal rates. In contrast, the electron-withdrawing derivatives are very effective at oxidizing peroxide but have difficulty binding the substrate so that maximal rates can be achieved only at high peroxide concentrations. Optimal efficiency, as measured by k_{cat}/K_M, occurs at a compromise between these two factors with the intermediate $[Mn^{III}(2\text{-}OHsalpn)]_2$ derivative.

These kinetic properties also explain how we have been able to observe different species in our experiments. We used the $[Mn^{III}(2\text{-}OH(3,5\text{-}Clsal)pn)]_2$ under low substrate conditions in a mixture of DMF/acetonitrile to observe the $[Mn^{II}(2\text{-}OH(3,5\text{-}Clsal)pn)]_2^{2-}$. Similarly, we resorted to the $[Mn^{II}(2\text{-}OH(5\text{-}NO_2\text{-}sal)pn)]_2^{2-}$ to detect the mixed-valent intermediate of the inactivation reaction discussed below which is too fleeting to be characterized with the more electron-donating derivatives.

The simplest mechanism that accounts for the spectroscopic evidence and observed kinetic behavior is that shown in Scheme 1. This mechanism also includes both the reduced and oxidized symmetric dimers as intermediates in the reaction. This is important since both $[Mn^{II}(2\text{-}OH(5\text{-}Clsal)pn)]_2^{2-}$ and $[Mn^{III}(2\text{-}OH(5\text{-}Clsal)pn)]_2$ exhibit saturation kinetics with identical kinetic parameters and show no lag phase, results which are consistent with each dimer being active in the catalytic cycle.

Mechanism of Inactivation. In addition to being an efficient functional model for the normal catalytic function of the Mn catalases, the $[Mn(2\text{-}OHsalpn)]_2$ system, when reacted with hydrogen peroxide under high oxygen concentrations, causes inactivation of the catalyst in a process that may present insights into the hydroxylamine-driven inactivation of the Mn catalase. The reaction of the $[Mn^{II}(2\text{-}OH(5\text{-}NO_2sal)pn)]_2^{2-}$ with excess H_2O_2 in a closed EPR tube causes a conversion to a catalytically inactive $Mn^{III/IV}$ dioxo-bridged dimer. Scheme 2 illustrates the proposed deactivation pathway. In step 1, the Mn^{II} dimer is

Scheme 2

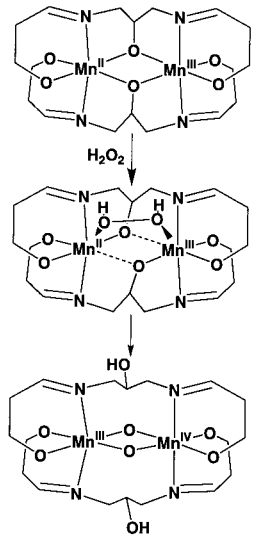

oxidized by one electron by the accumulation of dioxygen from the peroxide disproportionation reaction.

Those $Mn^{II}Mn^{III}$ dimers that again react with dioxygen form a Mn^{III} dimer[24] that rejoins the catalytic cycle; however, the $Mn^{II}Mn^{III}$ dimers that are intercepted by peroxide are irreversibly oxidized to the dioxo-bridged complex $[Mn^{III/IV}(2\text{-}OH(5\text{-}NO_2\text{-}sal)pn)_2(\mu_2\text{-}O)_2]^-$. Consistent with this proposal is the detection of an EPR signal in Figure 5F assigned to $[Mn^{II/III}(2\text{-}OH(5\text{-}NO_2sal)pn)_2]^-$.[24] Furthermore, stoichiometric addition of H_2O_2 will quantitatively convert $[Mn^{II/III}(2\text{-}OH(5\text{-}NO_2sal)pn)_2]^-$ to $[Mn^{III/IV}(2\text{-}OH(5\text{-}NO_2sal)pn)_2(\mu_2\text{-}O)_2]^-$ (see Figure S4, Supporting Information).

The catalase activity of a $[Mn^{III/IV}(2\text{-}OH(X\text{-}sal)pn)_2(\mu_2\text{-}O)_2]^-$ sample can be restored upon addition of hydroxylamine hydrochloride to the solution. The addition of an excess of solid hydroxylamine hydrochloride to a solution of $[Mn^{III/IV}(2\text{-}OH\text{-}(3,5\text{-}Clsal)pn)_2]ClO_4$ in acetonitrile reduced the $Mn^{III/IV}$ dimer to a catalytically active species. The rate of O_2 evolution was the same as that observed for the $[Mn^{III}(2\text{-}OH(3,5\text{-}Clsal)pn)]_2$ dimer at 300 mM H_2O_2. Similar results were observed for $[Mn^{III/IV}(2\text{-}OH(5\text{-}NO_2sal)pn)_2(\mu_2\text{-}O)_2]^-$. Addition of the solid hydroxylamine hydrochloride to the solution of $[Mn^{III/IV}(2\text{-}OH(5\text{-}NO_2sal)pn)_2(\mu_2\text{-}O)_2]^-$ restores over 80% of the catalase activity of the $[Mn^{III}(2\text{-}OH(5\text{-}NO_2sal)pn)]_2$ at 300 mM H_2O_2. While we have not studied this reaction quantitatively, it is clear that hydroxylamine will reduce all of the dimers (i.e., $[Mn^{II/III}\text{-}(2\text{-}OH(X\text{-}sal)pn)_2]^-$, $[Mn^{III}(2\text{-}OH(X\text{-}sal)pn)]_2$, $[Mn^{III/IV}(2\text{-}OH\text{-}(X\text{-}sal)pn)]_2^+$, $\{[Mn^{IV/IV}(2\text{-}OH(X\text{-}sal)pn)]_2OH\}^+$, $[Mn^{III/IV}(2\text{-}OH(X\text{-}sal)pn)_2(\mu_2\text{-}O)_2]^-$, and $[Mn^{IV}(2\text{-}OH(X\text{-}sal)pn)(\mu_2\text{-}O)]_2$) in this study to the $[Mn^{II}(2\text{-}OH(X\text{-}sal)pn)]_2^{2-}$ form. Thus, we believe that it is most likely that the initial reduction of $[Mn^{III/IV}\text{-}(2\text{-}OH(X\text{-}sal)pn)_2(\mu_2\text{-}O)_2]^-$ leads to the formation of $[Mn^{II}(2\text{-}OH(X\text{-}sal)pn)]_2^{2-}$ which is catalytically competent.

The reactions that have been shown for this versatile dimeric series $[Mn(2\text{-}OHsalpn)]_2^{2-,1-,0}$ are summarized in Figure 6. This figure shows the relationship of the structurally characterized dimers of 2-OHsalpn and their interconversion. This is the first dimer series that can address many of the mechanistic aspects of the Mn catalases since it is the only catalytically active series to be isolated and characterized crystallographically in more than one oxidation state and studied in such kinetic detail.

Relationship to the Mn Catalases. This reactivation is very similar to the chemistry observed for the Mn catalases. The

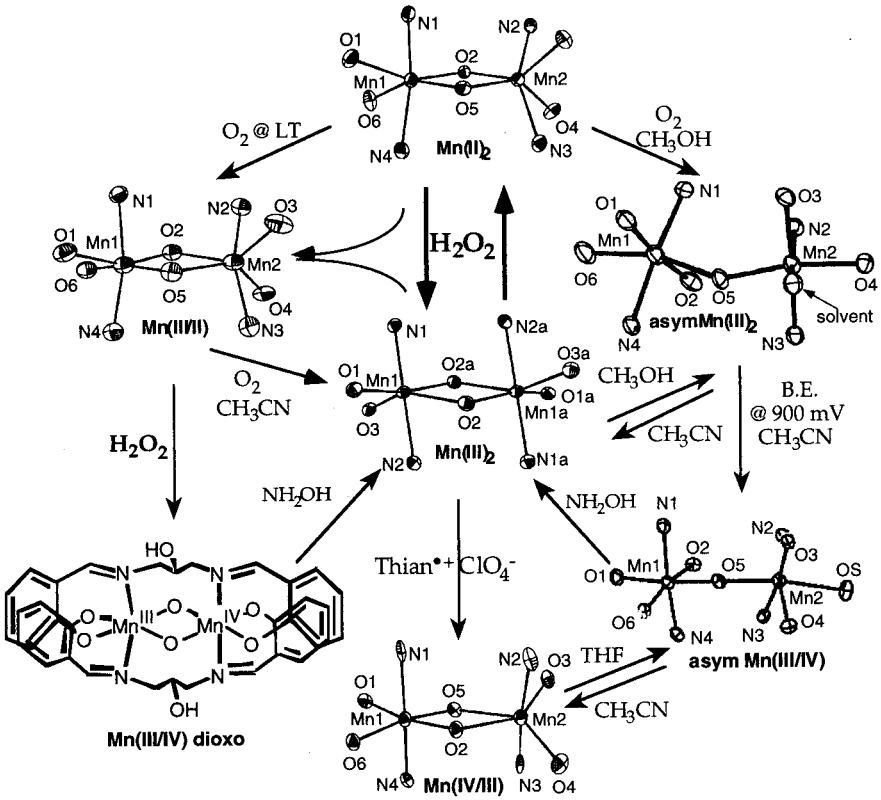

Figure 6. Cycle of interconversions between dimers as described in the text. All species have been crystallographically characterized except for the dioxo-bridged $Mn^{III/IV}$.

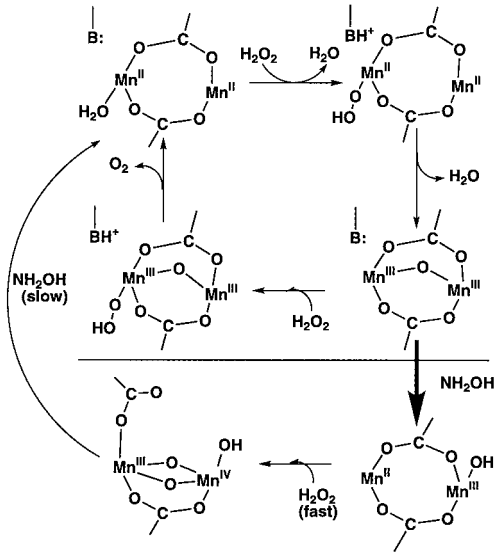

Figure 7. Modification of the kinetic cycle for the Mn catalase as proposed by Penner-Hahn et al. to include a pathway for enzyme deactivation. In the present proposal, a $Mn^{III}Mn^{III}$ enzyme form that is produced by the reduction of the $Mn^{III}Mn^{III}$ state by hydroxylamine is oxidized by two electrons using peroxide. This results in the catalytically inactive $Mn^{III}Mn^{IV}$ di-μ_2-oxo dimer. This superoxidized state can be reactivated by the addition of hydroxylamine in the absence of hydrogen peroxide. A version of this figure has previously appeared in Pecoraro, V. L.; Baldwin, M. J.; Gelasco, A. *Chem. Rev.* **1994**, *94*, 807−826.

inactive "superoxidized" Mn catalase can be reduced to the fully active state by long term incubation with hydroxylamine. Figure 7 shows a proposed mechanism for the inactivation of the Mn catalase based on the observations of this synthetic model. The top portion of the scheme is similar to the mechanism previously presented by Penner-Hahn.[7] The bottom portion shows a possible structural rearrangement that could occur under conditions that inactivate the Mn catalase. During turnover in the presence of hydroxylamine, the Mn^{III} catalase can react with NH_2OH to form the one-electron-reduced $Mn^{II/III}$ catalase, analogous to the formation of the one-electron-oxidized $[Mn^{II/III}(2\text{-}OHsalpn)_2]^-$. If next another NH_2OH molecule reacts with the $Mn^{II/III}$ catalase, the enzyme could be further reduced to the catalytically active Mn^{II}_2 form, and the catalytic cycle could continue. If, however, the $Mn^{II/III}$ catalase reacts with a peroxide molecule, then the enzyme is inactivated and forms a dioxo-bridged $Mn^{III/IV}$ species. While NH_2OH can reduce the $Mn^{III/IV}$ catalase, this reaction is slow, and the $Mn^{III/IV}$ enzyme becomes the dominant species present.

Acknowledgment. The authors thank Dr. M. T. Caudle, Dr. M. J. Baldwin, Mr. N. Law, and Mr. W.-Y. Hsieh for useful discussions. This work was funded by the National Institutes of Health grant GM 39406 to V.L.P.

Supporting Information Available: Supplemental Figures S1−S4 showing time-dependent electronic spectra, positive and negative FAB-MS, and EPR spectra (5 pages). Ordering information is given on any masthead page.

IC980022A